Feb 2017. Vol. 12. No. 01 ISSN 2305-8269
International Journal of Engineering and Applied Sciences

www.eaas-journal.org

CHARACTERIZATION AND GAS PERMEATION PROPERTIES OF POLYETHERIMIDE/ZEOLITIC IMIDAZOLATE FRAMEWORK-8 (PEI/ZIF-8) MIXED MATRIX MEMBRANES

[1]SENNUR DENIZ

[1]Assist. Prof., Department of Chemical Engineering, Yildiz Technical University, Istanbul-Turkey

E-mail: [1] deniz@yildiz.edu.tr

ABSTRACT

Zeolitic imidazolate frameworks (ZIFs) are a new class of nanoporous materials which can be synthesized with a wide range of pore sizes and used as nano fillers in mixed-matrix membranes (MMMs). In this work, ZIF-8 nanocrystals with potential of gas separation by adsorption were synthesized and used as filler for the preparation of MMMs for gas separation. ZIF-8 nanocrystals with 3.4 Å pore aperture were synthesized successfully and then polyetherimide (PEI) membranes containing ZIF-8 nanoparticles in different compositions (5, 10, 15 and 30 wt.%) were prepared using the solution casting method. ZIF-8 nanocrystals and PEI/ZIF-8 membranes were characterized by SEM, FTIR, BET and XRD analyses. Then, we reported the permeability and selectivity values of H_2, CH_4 and CO_2 pure gases across PEI/ZIF-8 membranes. The gas permeation measurements were carried out at 3±0.1 bar at 35 °C. In the last step of the study, we used Higuchi model to predict the performance of PEI/ZIF-8 MMMs. The gas permeation results of PEI/ZIF-8 MMMs showed the permeability values of H_2, CH_4 and CO_2 gases increased with increasing the loading of ZIF-8 nanocrystals. i.e. P_{H_2} of pure PEI membranes and PEI/ZIF-8-30 membranes were 2.4884 Barrer and 3.3500 Barrer, respectively. Also it was demonstrated that the incorporation of ZIF-8 particles increased both solubility and diffusion coefficients. However, the ideal selectivity of all gases decreased with increasing the ZIF-8 loading. i.e. α_{H_2/CO_2} of pure PEI and PEI/ZIF-8-30 membranes were 5.74 and 3.19, respectively.

Keywords: ZIF-8, Polyetherimide, Mixed matrix membrane, Gas Permeability, Higuchi model

1. INTRODUCTION

Researchers have revealed that the energy demand shows a 1.7% average annual growth in the period between 2005 and 2020 due to global population and industrialization [1, 2]. Although fossil fuels are essential and commonly used energy sources in the world, their pollutant emissions release to environment. However, penalizations through growing restrictions in pollutant emissions of coal (especially in Europe) promote researchers to search for new energy sources [1].

At this point, natural gas recovery attracts attention due to the fact that natural gas causes less pollution than fossil fuels such as oil and coal do [1]. Also in petrochemical-related industries, membrane technologies are being more widely used for their advantages [3]. Due to their requirement for lower energy, lower operating cost and smaller carbon footprint, membrane technologies become more prominent than the other separation technologies such as distillation, absorption and condensation do which require a phase change in the mixture to separate [4, 5].

In the membrane separation process, one of the driving forces (concentration or pressure) ensures transport of one or more components to be separated through the membrane [6]. Gas separation processes occur by means of four important methods including absorption, adsorption, cryogenics and membrane technology, which are based on different physical and chemical properties of the species [3]. When membrane technology is preferred, some properties are expected from the gas separation membranes for an efficient separation or purification process and the most important ones of these properties are high permeability, high selectivity, mechanical stability and low cost [5]. However, although permeability and selectivity are the two common basic parameters to specify the performance of gas separation, gas separation membranes have a trade-off between gas selectivity and permeability [3, 7]. In addition, shape of the molecules to be separated and their interaction with the membrane material are other parameters, which have an impact on gas separation through membranes [8].

Metal-organic frameworks (MOFs), which are a new class of microporous materials composed of transition metals and transition metal oxides connected by organic linkers, have high pore volumes, well-defined pores, large surface areas, specific adsorption affinities and a large variety of chemical structures [7,9,10]. The superior properties like these make MOFs candidates to use gas adsorption and storage, molecular separation, and catalysis applications [9].

Zeolite imidazolate frameworks (ZIFs), which are made up of tetrahedral networks that are similar to those of zeolites with transition metals connect by imidazolate ligands, are a new class of MOFs [7]. They can be commonly used in gas adsorption and storage, molecular separation and catalysis because of their high surface area, uniform pore structures and exceptional thermal and chemical stabilities [11, 12].

ZIF-8 with the formula $Zn(mim)_2$ (mim = 2-methylimidazolate) is the most extensively studied prototypical zeolitic imidazolate framework (ZIF) porous solids [13]. ZIF-8 exhibits high thermal (up to 400 °C) and chemical stabilities compared to other porous MOF materials [13, 14]. It is not only highly stable but also shows adsorption affinity toward hydrogen (kinetic diameter ~2.9 Å) and methane (kinetic diameter ~3.8 Å) [15]. ZIF-8 membranes can use to separate H_2 (kinetic diameter ~2.9 Å) from larger molecules (N_2, CH_4, O_2, CO_2, etc.) [12]. Also, flexible nature of ZIF-8 enables the adsorption of molecules larger than 3.4 Å [13].

There has been a growing interest in MMMs containing MOF fillers as seen in the literature reports [13,16,17,26-34]. Additionally, there have been a few reports in recent literature of MMMs containing a ZIF-8 [26,27,29,31,35].

In this work; ZIF-8 nanofillers were synthesized successfully and then incorporated in PEI polymer (Ultem® 1000), which is a well-known class of engineering thermoplastic and has excellent thermal, chemical and mechanical stabilities [16], with the five different concentrations (0, 5, 10, 15 and 30 wt.%). After the characterization procedures by XRD, FTIR and SEM, the prepared membranes were used for gas permeation tests at 3±0.1 bar and 35 °C.

2. THEORY

Gas permeation properties of mixed matrix membranes (MMMs) were used to theoretically make predictions through several different models. Among these are the Maxwell, Higuchi, Bruggeman, Lewis-Nielsen and Bottcher-Landauer models. These models are developed for different conditions. The Bottcher-Landauer and Lewis-Nielsen models are originally developed for electrical resistance of binary metallic mixtures and elastic modules of particulate composites, respectively [17, 18]. The Bruggeman model, which is used for estimating gas permeability at high filler volume fraction, is originally developed for dielectric constant of particulate composites [17].

The Maxwell model is the best-known one among them. Maxwell presented the Eq. 1 in 1873 to predict the conduction of a dielectric through heterogeneous media and now it is often used for membranes filled with spherical particles [19, 20].

$$Peff = Pc\frac{Pd + 2Pc - 2\phi\,(Pc - Pd)}{Pd + 2Pc - \phi\,(Pc - Pd)} = Pc\frac{2\,(1-\phi) + \alpha\,(1+2\phi)}{(2+\phi) + \alpha\,(1-\phi)} \quad (Eq.1)$$

$$\alpha = \frac{Pd}{Pc} \quad (Eq.2)$$

$$\beta = \frac{\alpha - 1}{\alpha + 2} = \frac{Pd - Pc}{Pd + 2Pc} \quad (Eq.3)$$

where P_{eff} is the effective permeability of the composite membrane, ϕ is the volume fraction, β is the reduced permeation polarizability and lastly P_c and P_d represent the permeability of the continuous phase (polymer, PEI) and dispersed phase (filler, ZIF-8), respectively.

The Maxwell model equation cannot be used for mixed matrix membranes at the maximum packing volume fraction of filler particles. This model is applicable for low particle loadings (when volume fraction is less than about 20%). In addition to this, the Maxwell model does not take into account particle agglomeration, particle size distribution and particle shape [17].

The Higuchi model (given in Eq. 4) is applicable when spherical particles are randomly dispersed in membranes.

$$P\,eff = Pc\left[1 + \frac{3\,\emptyset d}{\frac{Pd + 2\,Pc}{Pd - Pc} - \emptyset d - K\left[\frac{(1 - \emptyset d)(Pd - Pc)}{Pd + 2\,Pc}\right]}\right] \quad (Eq.4)$$

where K is an empirical constant and is generally assigned a value of 0.78 on the basis of experimental data [18].

3. EXPERIMENTAL STUDY:

3.1 Materials

Polyetherimide (PEI, Ultem® 1000) was provided by GE Plastics, and n-methyl-2-pyrrolidone (NMP),

Zinc nitrate hexahydrate [$Zn(NO_3)_2.6H_2O$] and 2-methylimidazole [$C_4H_6N_2$] were all obtained from Acros Organics and methanol, which was used as a solvent, produced by J.T. Baker. The chemical structures of PEI and ZIF-8 are given in Fig. 1. High purity gases of H_2, CH_4 and CO_2 were used for the gas permeation experiments.

Figure 1. Chemical structures of PEI and ZIF-8 [5,20].

3.2 ZIF-8 nanoparticle synthesis

The ZIF-8 nanoparticles were synthesized through a modified recipe reported by Song et al. (the rapid room temperature synthesis method) [20]. In this method, two prepared methanol solutions, (25 ml methanol - 0.367 g, 1.23 mmol Zinc nitrate hexahydrate) and (25 ml methanol - 0.811 g, 9.89 mmol 2-methylimidazole), were mixed. Then, this colorless crystalline solution was mixed by a magnetic stirrer for 1 h at room temperature. After 1 h stirring, the product was separated by using centrifugation, followed by washing with methanol three times and finally redispersing as crystals in fresh methanol for use in membrane preparation. The yield of ZIF-8 was about 40 mol% based on the ideal molar conversion of zinc.

3.3 Preparation of PEI/ZIF-8 Mixed Matrix Membranes

The Ultem® 1000 polymer (PEI) was dried in a vacuum oven at 110 °C overnight. Firstly, for pure PEI membrane preparation, PEI pellets were dissolved in n-methyl-2-pyrrolidone at room temperature to give a 10 wt.% solution and stirred for 1-2 days until a clear solution was obtained. MMMs containing 5, 10, 15 and 30 wt.% ZIF-8 in Ultem® 1000 were fabricated by mixing a dispersion of ZIF-8 by using the Eq. (5). The MMMs solutions were stirred for two days at room temperature. Before casting, the solutions were sonicated to remove the air bubbles. After sonication, the resulting PEI/ZIF-8 solutions were drop-cast onto petri dishes with membrane thickness to be in the range between 80-100 μm at atmospheric conditions. After that, the casting membranes were placed in a vacuum oven at 50°C for 24 h and then at 70°C for 24 h to evaporate the solvent slowly. Finally, MMMs were annealed at 90 °C for 2 h, 120 °C for 2 h, and 200 °C for 2 h under vacuum before slow cooling to room temperature; all membranes were stored dry prior to gas permeation and structure characterization. The ZIF-8 loading in MMMs was defined as follows:

$$ZIF-8\ loading = \frac{wZIF-8}{wZIF-8+\ wpolymer}\ x\ 100 \qquad (Eq.5)$$

3.4 Characterization of Membranes

The volume fraction Φ_D of ZIF-8 in the nanocomposite membrane is defined as:

$$\Phi_D = [m_D/\rho_D] / [m_D/\rho_D + m_C/\rho_C] \qquad (Eq.\ 6)$$

where m and ρ refer to the mass and density of the continuous phase (polymer) and dispersed phase (ZIF-8), respectively, denoted by subscripts ''C'' and ''D''.

Characterization of morphological structures of ZIF-8 and PEI/ZIF-8 mixed matrix membranes was conducted on a JSM 6400 Scanning Electron Microscope (SEM). Samples were prepared by freeze fracture of the membrane and subsequent sputter-coating with a thin layer of gold.

The wide angle X-ray diffraction (XRD) was performed with a Rigaku D/max-2200 Ultima X-ray diffractometer using Cu Kα radiation with a step of 0.02° s^{-1}. The membrane sample was attached onto a sample holder with a single crystal silicon substrate.

Fourier transform infrared spectroscopy (FTIR) was performed on a NICOLET FTIR (iS10, Thermo Scientific) over the wavelength range of 400-4000 cm^{-1}. The thin mixed matrix membrane films and ZIF-8 nanocrystals were used directly, both under the transmission mode.

The specific surface area and pore size distribution of the ZIF-8 nanoparticles were determined from the nitrogen adsorption isotherms at 77 K (Micromeritics ASAP 2020). ZIF-8 sample was degassed under high vacuum (<10^{-6} bar) for 4 h prior to the measurement. The specific surface area (SBET) was calculated based on the Brunauer-Emmett-Teller (BET) model and the pore volume was derived from the BJH Adsorption model.

3.5. Gas permeation test

The pure gas (H_2, CH_4 and CO_2) permeability tests of the prepared composite membrane were carried out at 35±0.01°C. The prepared PEI/ZIF-8 membrane was put into a stainless steel permeation cell. Also the Viton™ gaskets were used to prevent any gas leak and the systems had pressure and temperature controllers (Fig. 2). The permeation temperatures of the cells were controlled by a temperature controller with a heating tape and the pressure changes were measured by precision pressure sensors. In addition, the precision-controlled constant temperature cabinets were used to keep the temperature constant. The measurement of gas permeability was realized by constant volume/variable pressure. In this method, the bottom area of the membrane cell was vacuumed and the feed gas (3±0.1bar) to be measured in the membrane was taken from the expansion tank. The pressure changes were transferred to computer with a convertor. The permeability values of each gas in the membrane were calculated with pressure values that were saved and the diffusion and solubility coefficients were calculated via time-lag method.

Two main characteristics used for comparison of membrane performances are selectivity and flow passing through the membrane. The latter, often defined as permeation rate (*P*), is denoted as the amount of the gas flowing through the membrane per unit area and time (Eq.7).

$$P = \frac{Ji \; x \; l}{\Delta Pi} \qquad (Eq.7)$$

where *Ji* is the flux of permeating gas *i*, *l* is the thickness of the particular membrane and Δ*Pi* is the effective partial pressure difference of species *i* across the membrane meaning transmembrane pressure difference. The permeabilities are commonly defined as are in the unit of Barrer:

$$Barrer = 1x10^{-10} \frac{cm^3(STP)\,cm}{cm^2 \; S \; cmHg} \qquad (Eq.8)$$

While the gas is passing through dense polymeric membranes, gas penetrants adsorb into the membrane from the upstream feed and then diffuse through the membrane to the downstream permeate with the driving force. This transport situation can be described by the solution-diffusion mechanism [21]. Permeability calculation can be written as shown in Eq. 9 below:

$$Pi = Di \; x \; Si \qquad (Eq.9)$$

Selectivity (α) is the indication of separation ability of a membrane. Ideal selectivity is the ratio of permeabilities of two single gases. It depends on the experimental conditions, such as pressure differences of the applied gases.

$$\alpha i/y = \frac{Pi}{Py} \qquad (Eq.10)$$

4. RESULTS AND DISCUSSION

4.1. Characterization of ZIF-8 nanocrystals and PEI/ZIF-8 mixed matrix membranes

4.1.1. Powder X-ray diffraction (XRD)

XRD peaks' sites and intensities of all crystals, which are seen in Fig. 3, correspond to sodalit topology of ZIF-8 and these peaks of ZIF-8 crystals are also obtained according to literature in terms of their structural stability [20, 22]. Also, a very sharp peak below 10° (with 2θ of 7.2) seen on XRD diffractogram of the ZIF-8 indicate that ZIF-8 material was synthesized at highly crystalline structure.

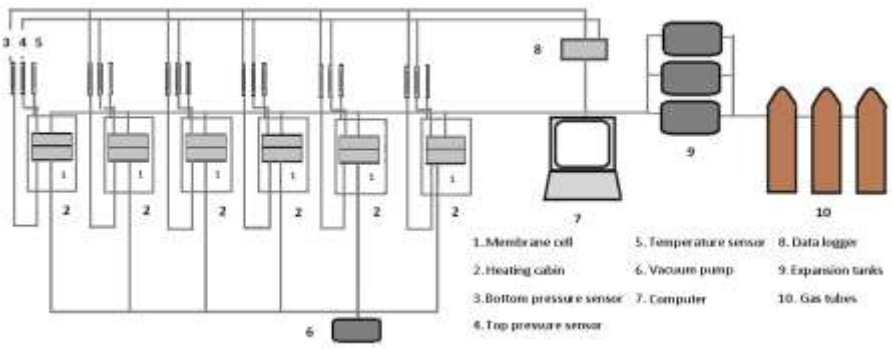

Figure 2. Schematic diagram of gas permeation set up.

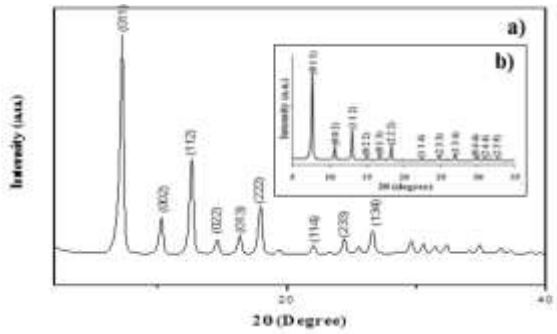

Figure 3. XRD pattern of ZIF-8 crystal a) characterization result of this study b) ref [22].

4.1.2. Determination of the surface area and pore volume of the ZIF-8 nanocrystals

The pore size and surface area of the ZIF-8 nanocrystals were determined by N_2 adsorption at 77 K on ZIF-8. Fig. 4 shows a Type I isotherm, which is indicative of a microporous material. Multipoint BET surface area (1413 m^2/g) was obtained by using the P/P_o data points ranging from 0.01-0.10 along the curve of the isotherm plot, which correspond to the formation of a monolayer of adsorbate molecules. The pore volume of the ZIF-8 nanocrystal material was determined to be 0.4744 cm^3/g. It could be said that the BET surface areas of ZIF-8 crystals in this study conformed to the surface area values in literature [20, 24, 26].

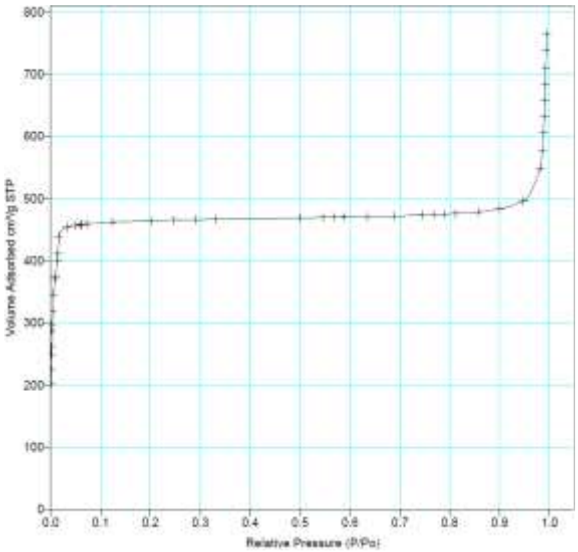

Figure 4. N_2 adsorption isotherm of the ZIF-8. The ZIF-8 nanocrystals were annealed at 60 °C and 230 °C respectively under high vacuum for 18 h prior to N_2 adsorption measurements at 77 K.

4.1.3. Fourier–transform infrared spectroscopy (FTIR)

FT-IR spectra of ZIF-8 were recorded at room temperature. These spectra were collected at the wave number between 650 cm^{-1} and 4000 cm^{-1} with spectral resolution of 1 cm^{-1}. It is decided according to Fig. 5 that the peak around 1580-1585 cm^{-1} is infrared band of C=N links, the other two characteristic stretching bands of C-N links are seen at 1145 cm^{-1} and 990 cm^{-1} wavelengths. The synthesized ZIF-8 crystals show that they conform to literature when all of these results are evaluated [23, 24]. However, an inconsistency arose between synthesized ZIF-8 and literature. The explicit peaks were formed around 3400-2200 cm^{-1} in Fig. 5. The stretching, which is seen at this aperture, is generally a characteristic structure of N-H band [25]. It was decided about this part of the spectrum that 2-methyl imidazole did not completely react.

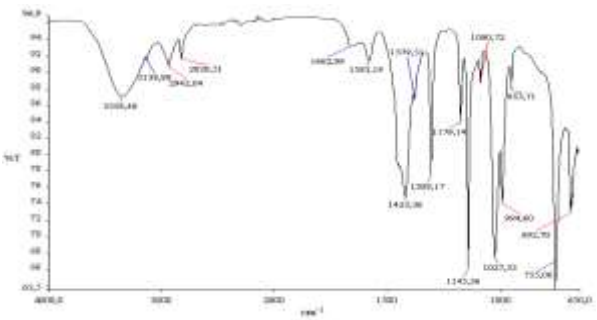

Figure 5. The FTIR spectra of ZIF-8.

4.1.3. Scanning electron microscopy (SEM)

Characterization studies of ZIF-8 nanocrystals and PEI/ZIF-8 membranes morphologies were conducted on a JSM 6400 Scanning Electron Microscope (SEM). Fig. 6 revealed spherical-like particles of similar size. In the pre-procedure of SEM characterization, all of the membranes were fractured by using liquid nitrogen to give a generally consistent cross sectional view. It can be said regarding the SEM results that the synthesized ZIF-8 crystals are well-shaped spherical-structured and their sizes are about 50 nm.

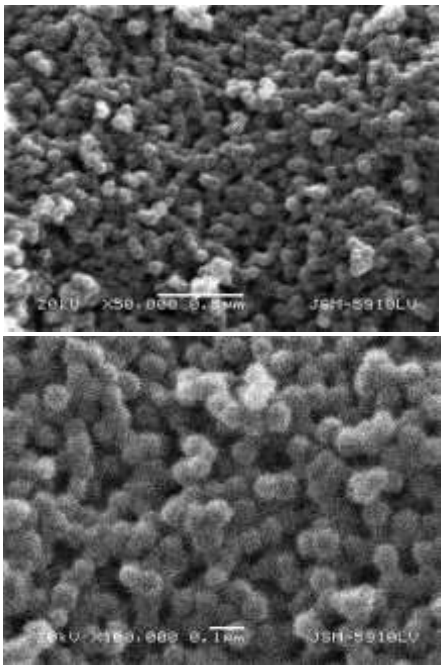

Figure 6. SEM images of ZIF-8 for different magnifications.

SEM was used to study the membrane cross section morphology as well as probe the particle-polymer interface. Sample images from 30 wt.% ZIF-8 loaded PEI/ZIF-8-30 membranes were shown in Fig. 7. SEM images of the dense film membrane cross sections showed a homogeneous dispersion of the ZIF-8 material in the polymer matrix and good adhesion between the ZIF-8 and polymer. This uniform dispersion and good adhesion indicated that the polymer and ZIF-8 were compatible. Furthermore, the dispersion of the sieve in the polymer matrix was quite sufficient (limited agglomerates present), suggesting that the PEI/ZIF-8 MMMs produced the desired morphology

4.2. Gas permeation of PEI/ZIF-8 MMMs

Mixed matrix membranes with ZIF-8 loading were fabricated using PEI (Ultem® 1000) as polymer matrix. The pure component H_2, CH_4 and CO_2 gas permeation performances of PEI/ZIF-8 nanocomposite membranes and the relationship between these performances and the kinetic diameters of gases are summarized in Table 1 and Fig. 8. The gas permeabilities considerably depend on the kinetic diameters of gases and Fig. 8 indicated this idea. Therefore the permeations of H_2 and CO_2 are expected to be higher than that of CH_4. Also it can be expected that the permeability results of H_2 and CO_2 gases increase with ZIF-8 loading.

Table 1. Gas permeabilities (Barrer) of the pure PEI and PEI/ZIF-8 mixed matrix membranes at 35°C and 3 bar.

PEI/ZIF-8	Permeability, P *(Barrer)*		
	P_{H2}	P_{CH4}	P_{CO2}
PEI/ZIF-8-0	2.4884	0.0278	0.4333
PEI/ZIF-8-5	2.6313	0.0458	0.5810
PEI/ZIF-8-10	2.7400	0.0562	0.6153
PEI/ZIF-8-15	3.1511	0.0832	0.8143
PEI/ZIF-8-30	3.3500	0.1445	1.0490

Bux et al. have mentioned a relationship between the permeabilities and the kinetic diameters of gases and commented as follows: kinetic diameter of CH_4 (~0.38) is higher than the pore size of ZIF-8 (~0.34 nm), however, CH_4 can pass through the pore network, and consequently, there exists no sharp cutoff at 0.34 nm. They have attributed this situation to the fact that the framework structure of ZIF-8 is in fact more flexible rather than being static in its nature [15]. Thus, the ZIF-8 pore aperture allows it to readily adsorb H_2, CH_4 and CO_2 molecules

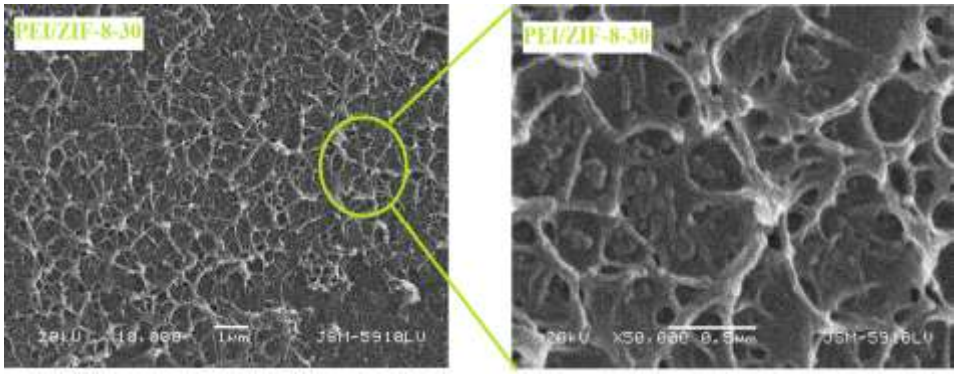

Figure 7. SEM images of PEI/ZIF-8-30 mixed matrix membranes for different magnifications.

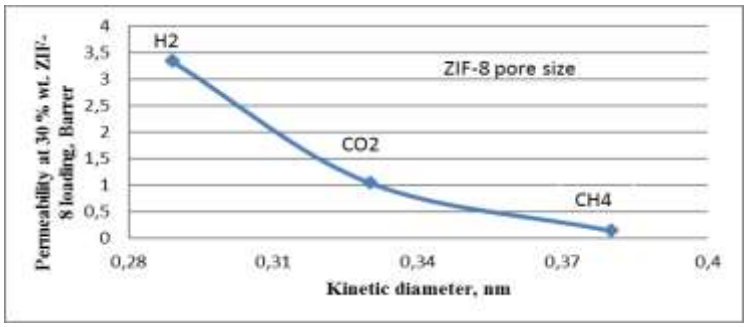

Figure 8. Pure gas permeabilities for PEI/ZIF-8-30 membrane vs. kinetic diameters of gases.

and the permeability values of all gases increased as the ZIF-8 loading increased to 30% (w/w). For example, CH_4 permeability of PEI/ZIF-8 (30 wt.%) membrane was five times higher than the permeability of pure PEI membrane and the increases in other gas permeabilities were between 1.5 and 2.5 times.

As shown in Table 1 and 2, the change of ideal gas selectivities occurred as the inverse of permeabilities. For example; at the 30 wt.% ZIF-8 loading P_{H2}, P_{CH4} and P_{CO2} of pure PEI membrane increased from 2.4884 to 3.350 Barrer, 0.0278 to 0.1445 Barrer and 0.4333 to 1.0490 Barrer, respectively. However, when ZIF-8 nanocrystals was incorporated into PEI at 30 wt.% loading, the $\alpha_{H2/CH4}$, $\alpha_{H2/CO2}$ and $\alpha_{CO2/CH4}$ ideal selectivities of pure PEI membrane decreased by 77%, 44% and 58%, respectively under the same conditions.

PEI/ZIF-8-30 mixed matrix membranes showed a 420% enhancement in CH_4 permeability along with a 58% decrease in CO_2/CH_4 selectivity compared to pure PEI membranes. Shah et al. commented on a graph about CO_2/CH_4 selectivity vs. CO_2 permeability for different types of membranes [4]. According to this figure, ZIF-8 membrane showed relatively high CO_2 permeability, though the CO_2/CH_4 selectivity is relatively low. However, the CO_2 permeability increased as the CO_2/CH_4 selectivity decreased, or vice versa, because the pore size of ZIF-8 (0.34 nm) is slightly larger than the kinetic diameter of CO_2 (0.33 nm). Also Shah et al. [4] stated that a 3.4 aperture diameter leads to an expectation that ZIF-8 membranes would be capable of good H_2/CH_4 separation. The separation factors seen in Table 3 partially confirm this idea. Although the gas separation factors of ZIF-8 MMMs decrease with ZIF-8 loading, the most well-advised separation performance among the studied gas pairs (H_2/CH_4, H_2/CO_2, CO_2/CH_4) is seen to be that of H_2/CH_4 gas pair.

The researchers also compare ZIF-8 and MOF particles in terms of the performance of gas separation membranes. Basu et al. studied on the influence of three different MOFs in MMMs for binary gas mixture separations (CO_2/CH_4 and CO_2/N_2 mixtures at different CO_2 concentrations) by preparing dense and asymmetric Matrimid® membrane filled with/$[Cu_3(BTC)_2]$, ZIF-8 and MIL-53(Al). Consequently, the selectivity and permeance of CO_2/CH_4 and CO_2/N_2 feeds under different CO_2 compositions increased with increasing filler loading. Also HKUST-1 and MIL-53(Al) MMMs showed higher CO_2/CH_4 selectivity than ZIF-8 MMM. They stated that the increases in selectivity for HKUST-1 and MIL-53(Al) MMMs were attributed to the strong CO_2 interaction with the metal sites and nano filler interactions with the hydroxyl groups of the framework, respectively [26].

Table 2. Pure gas ideal separation factor for PEI/ZIF8 MMMs at 35°Cand 3 bar.

PEI/ZIF-8	$\alpha^P_{i,j} = P_i/P_j$			$\alpha^D_{i,j} = D_i/D_j$	$\alpha^S_{i,j} = S_i/S_j$
	$\alpha^P_{H2/CH4}$	$\alpha^P_{H2/CO2}$	$\alpha^P_{CO2/CH4}$	$\alpha^D_{CO2/CH4}$	$\alpha^S_{CO2/CH4}$
PEI/ZIF-8-0	89.40	5.74	15.57	1.86	10.54
PEI/ZIF-8-5	57.42	4.53	12.68	1.77	7.23
PEI/ZIF-8-10	48.73	4.45	10.94	1.69	6.01
PEI/ZIF-8-15	37.01	3.87	9.56	1.64	5.85
PEI/ZIF-8-30	20.82	3.19	6.52	1.60	5.12

The diffusion and solubility coefficients of all gases (H_2, CH_4 and CO_2), which contribute to the separation factor for membrane-based gas separations, are shown in Table 3. It is seen that the diffusion and solubility coefficients of all gases calculated by time-lag method increased with ZIF-8 loading. The diffusion coefficients of gases are mostly dependent on the kinetic diameter (H_2, 2.89 Å < CO_2, 3.3 Å < CH_4, 3.8 Å), while the solubility of gases in the polymer is strongly dependent on the thermodynamic affinity of the molecule on the membrane surface. The one of the ways of improving the performance of MOF/ZIF based polymer gas separation membranes may be alteration of the pore size by means of side groups on the organic linkers concerning the gaseous diffusion. However these side groups can enhance gas solubility changing thermodynamic interaction or sorption behavior of membrane [4]. When we look at the Table 3, it is seen that H_2 diffusion coefficients increased almost four times and CH_4 and CO_2 diffusion coefficients increased two times for PEI/ZIF-8-30 membranes compared to pure membranes. Also, H_2 and CH_4 solubility coefficients increased more than those of CO_2 did. S_{H2}, S_{CH4} and S_{CO2} increased from 4.943 to 10.697 x 10^6 m^3 (STP) cm^{-3} atm^{-1}, 1.627 to 5.329 x 10^6 m^3 (STP) cm^{-3} atm^{-1} and 17.146 to 27.289 x 10^6 m^3 (STP) cm^{-3} atm^{-1}, respectively at 30 wt.% ZIF-8 loading. According to these results, it can be summarized that the H_2 and CO_2 permeabilities were enhanced due to porosity of ZIF-8 by increased diffusion coefficients and CH_4 permeability was enhanced due to strong adsorption affinity by increased solubility coefficient. Partly similarly Bux et al. expressed that ZIF-8 is highly stable and it shows strong adsorption affinity toward H_2 and CH_4 gases [15].

Table 3. Diffusion and solubility coefficients of the pure PEI and PEI/ZIF-8 mixed matrix membranes at 35°C and 3 bar.

PEI/ZIF-8	*Diffusion coefficient, D* *(x 10^{-8} cm^2/s)*			*Solubility coefficient, S* *(x 10^6 $m^3(STP)/cm^3.atm$)*		
	D_{H2}	D_{CH4}	D_{CO2}	S_{H2}	S_{CH4}	S_{CO2}
PEI/ZIF-8-0	28.444	1.044	1.945	4.943	1.627	17.146
PEI/ZIF-8-5	28.945	1.807	3.190	5.868	2.559	18.501
PEI/ZIF-8-10	43.041	2.231	3.760	6.410	4.148	24.943
PEI/ZIF-8-15	53.948	2.336	3.840	7.037	4.338	25.358
PEI/ZIF-8-30	80.628	2.697	4.323	10.697	5.329	27.289

The permeability, diffusion and solubility coefficients of PEI/ZIF-8 nanocomposite membranes relative to pure PEI membranes for all gases are seen in Fig. 9. It can be seen that incorporating the ZIF-8 filler leads to an increase in not only diffusion and solubility coefficients, but also the gas permeability. Also we can say about H_2 and CO_2 that the relative permeability is strongly affected by the diffusion coefficient and less affected by the solubility coefficient. For CH_4, the relative permeability is affected more by the solubility coefficient than it is by diffusion coefficient.

4.5. Modeling of gas permeability in MMMs

As shown by Higuchi models in Fig. 10, the incorporation of permeable ZIF-8 nanocrystals into a polymer membrane led to an increase in the permeability of gases compared to the pure polymer membrane.

In our study, the kinetic diameters of H_2 and CO_2 are smaller than the ZIF-8 pore size and it was accepted that $P_d >> P_c$. Thus, when the Eq. (4) is rearranged, the calculations of the permeabilities of H_2 and CO_2 have to be strictly based on Eq. 11 and Eq. 12.

$$P\,\text{eff} = 2.4884 + \frac{7.4652\ \text{Ød}}{[1 - \text{Ød} + K\,[1 - \text{Ød}]]} \qquad (Eq.11)$$

$$P\,\text{eff} = 0.4333 + \frac{1.2999\ \text{Ød}}{[1 - \text{Ød} + K\,[1 - \text{Ød}]]} \qquad (Eq.12)$$

The kinetic diameter of CH_4 is close to the ZIF-8 pore size. Therefore $P_d >> P_c$ is not applicable here and P_d is calculated by Eq. 13 [18].

$$Pd = 97\,(\frac{r\,\varepsilon}{\tau})\,\frac{1}{R\,\sqrt{T\,M}}\ (\text{mol.m}^{-1}.\text{s}^{-1}.\text{Pa}^{-1}) \qquad (Eq.13)$$

where r is the mean pore diameter (m), ε is the porosity, τ is the tortuosity, R is the gas constant ($J.mol^{-1}.K^{-1}$), T is the absolute temperature, and M is the molecular weight.

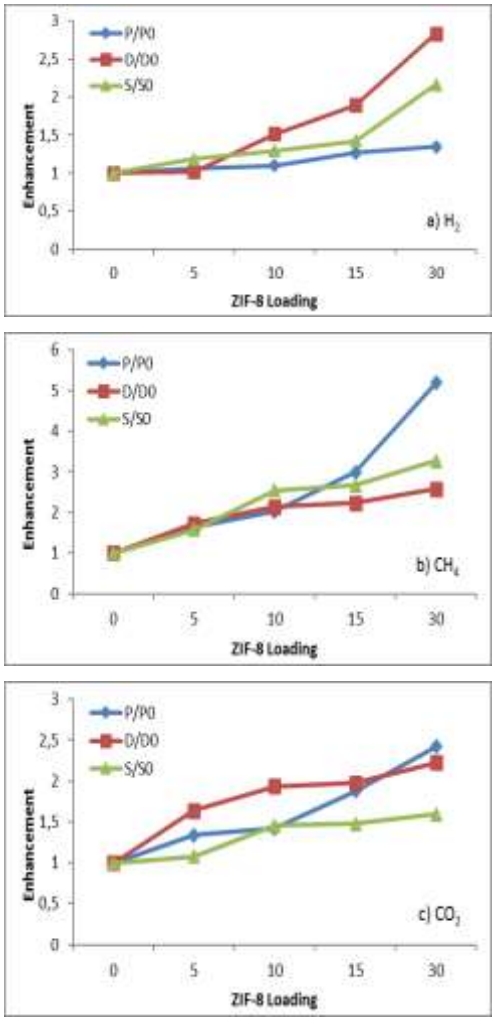

Fig. 9. Enhancement of gas transport properties for (a) H_2, (b) CH_4, and, (c) CO_2 as a function of ZIF-8 loading; enhancement in permeability coefficient (♦), diffusion coefficient (▲), and solubility coefficient (■).

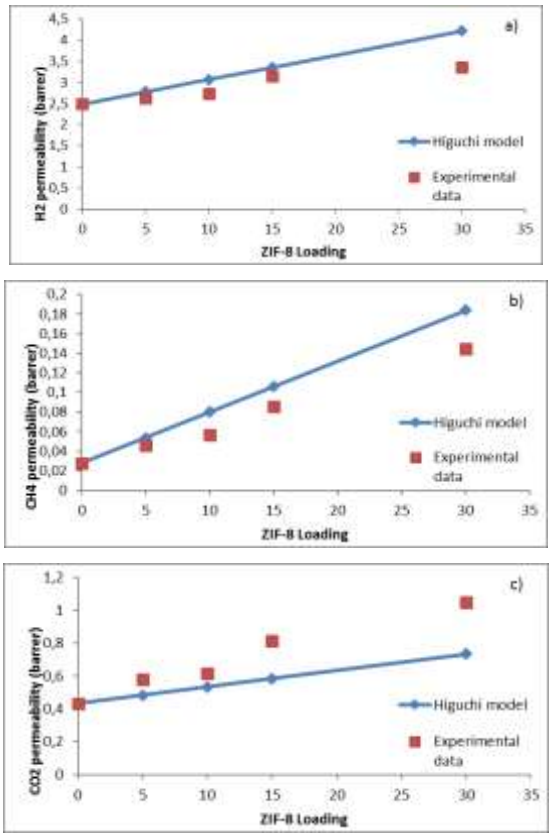

Fig. 10. Correlation of permeability coefficient to Higuchi model for (a) H_2, (b) CH_4, (c) CO_2.

4. CONCLUSION

In this study, ZIF-8 nanocrystals were synthesized and successfully incorporated into polyetherimide (Ultem® 1000) polymer matrix with various filler contents. Also the ZIF-8 nanocrystals and prepared membranes were characterized, their gas permeation tests were measured for H_2, CH_4 and CO_2 gases and finally separation factors and diffusion/solubility coefficients were calculated.

To sum up the results: XRD peaks' sites and intensities of all crystals correspond to sodalit topology of ZIF-8. The SEM results showed that the synthesized ZIF-8 crystals are spherical-structured and their sizes are about 50 nm.

According to the single gas permeation experiments, gas permeations increased with ZIF-8 loading to pure PEI membrane based on the kinetic diameter of gases. The H_2 (kinetic diameter is ~0.289 nm) permeation value is seen to be higher than CH_4 (kinetic diameter is ~0.38 nm) and CO_2 (kinetic diameter is ~0.33 nm) permeations. Also the permeations of all gases through MMMs were fitted in Higuchi model. However, while the change of ideal gas selectivities occurred as the inverse of ZIF-8 loading and diffusion and solubility coefficients increased with ZIF-8 loading. Also, we decided that H_2 and CO_2 permeabilities were enhanced due to the porosity of ZIF-8 and CH_4 permeability was enhanced due to the strong adsorption affinity. Lastly, the relative permeability of H_2 and CO_2 are strongly affected by the diffusion coefficient and less affected by the solubility coefficient. For CH_4, the relative permeability is affected more by the solubility coefficient than by diffusion coefficient.

Acknowledgments

This work was supported by Project of Yildiz Technical University Research Foundation under Project No. YTU-BAPK-2012-07-01-01-KAP04.

REFERENCES

[1] M. Tagliabue, D. Farrusseng, S. Valenciac, S. Aguado, U. Ravon, C. Rizzo, A. Corma, C. Mirodatos, "Natural gas treating by selective adsorption: Material science and chemical engineering interplay", Chem. Eng. J. 155 (2009), 553-566.

[2] J.-R. Li, Y. Ma, M. C. McCarthy, J. Sculley, J. Yu, H.-K. Jeong, P. B. Balbuena, H.-C. Zhou, "Carbon dioxide capture-related gas adsorption and separation in metal-organic frameworks", Coord. Chem. Rev. 255 (2011), 1791–1823.

[3] M. T. Ravanchi, T. Kaghazchi, A. Kargari, "Application of membrane separation processes in petrochemical industry: a review", Desalination 235 (2009), 199–244.

[4] M. Shah, M. C. McCarthy, S. Sachdeva, A. K. Lee, and H.-K. Jeong, "Current Status of Metal Organic Framework Membranes for Gas Separations: Promises and Challenges", Ind. Eng. Chem. Res. 51 (2012), 2179–2199.

[5] T.H. Bae, "Engineering Nanoporous Materials For Application In Gas Separation Membranes", School of Chemical & Biomolecular Engineering, PhD Dissertation, Georgia Institute of Technology, Atlanta (2010).

[6] P. S. Goh, A. F. Ismail, S.M. Sanip, B.C. Ng, M. Aziz, "Recent advances of inorganic fillers in mixed matrix membrane for gas separation", Sep. Purif. Technol. 81 (2011), 243–264.

[7] G. Yilmaz and S. Keskin, "Predicting the Performance of Zeolite Imidazolate Framework/Polymer Mixed Matrix Membranes for CO_2, CH_4, and H_2 Separations Using Molecular Simulations", Ind. Eng. Chem. Res. 51 (2012), 14218−14228.

[8] B. Zornoza, C. Tellez, J. Coronas, J. Gascon, F. Kapteijn, "Metal organic framework based mixed matrix membranes: An increasingly important field of research with a large application potential", Mic. Mes. Mater. 166 (2013), 67–78.

[9] A. Huang, H. Bux, F. Steinbach, and J. Caro, "Molecular-Sieve Membrane with Hydrogen Permselectivity: ZIF-22 in LTA Topology Prepared with 3-Aminopropyltriethoxysilane as Covalent Linker", Angew. Chem. Int. Ed. 49 (2010), 4958 –4961.

[10] V. V. Guerrero, "Nanoporous Materials for Carbon Dioxide Separation and Storage", Materials Science and Engineering, PhD Dissertation, Texas A&M University (2011).

[11] F.-K. Shieh, S.-C. Wang, S.-Y. Leo, and K. C.-W. Wu, "Water-Based Synthesis of Zeolitic Imidazolate Framework-90 (ZIF-90) with a Controllable Particle Size", Chem. Eur. J. 19 (2013), 11139 – 11142.

[12] J. O. Hsieh, "Mil-53 Frameworks in Mixed-Matrix Membranes and Cross-Linked ZIF-8/Matrimid® Mixed-Matrix Membranes for Gas

Separation", PhD Dissertation, The University of Texas, Dallas (2010).

[13] S. Sorribas, B. Zornoza, C. Téllez, J. Coronas, "Mixed matrix membranes comprising silica-(ZIF-8)core–shell spheres with ordered meso–microporosity for natural-and bio-gas upgrading", J. Membr. Sci. 452 (2014), 184–192.

[14] F. Cacho-Bailo, B. Seoane, C. Téllez, J. Coronas, "ZIF-8 Continuous Membrane on Porous Polysulfone for Hydrogen Separation", J. Membr. Sci 464 (2014), 119-126.

[15] H. Bux, F. Liang, Y. Li, J. Cravillon, M. Wiebcke and J. Caro, "Zeolitic Imidazolate Framework Membrane with Molecular Sieving Properties by Microwave-Assisted Solvothermal Synthesis", J. Am. Chem. Soc. 131 (2009), 16000–16001.

[16] S. Saimani, A. Kumar, M. M. Dal-Cin, G. Robertson, "Synthesis and characterization of bis (4-maleimidophenyl) fluorene and its semi interpenetrating network membranes with polyether imide (Ultem® 1000)", J. Membr. Sci. 374 (2011), 102–109.

[17] M. A. Aroon, A. F. Ismail, T. Matsuura, M. M. Montazer-Rahmati, "Performance studies of mixed matrix membranes for gas separation: A review", Sep. Purif. Technol. 75 (2010), 229–242.

[18] Y. Shen and A. Chong Lua, "Theoretical and Experimental Studies on the Gas Transport Properties of Mixed Matrix Membranes Based on Polyvinylidene Fluoride", AIChE J. 59 (2013), 4715–4726.

[19] H. Cong, M. Radosz, B. F. Towler, Y. Shen, "Polymer–inorganic nanocomposite membranes for gas separation", Sep. Purif. Technol. 55 (2007), 281–291.

[20] Q. Song, S. K. Nataraj, M. V. Roussenova, J. C. Tan, D. J. Hughes, W. Li, P. Bourgoin, M. A. Alam, A. K. Cheetham, S. A. Al-Muhtaseb and E. Sivaniah, "Zeolitic imidazolate framework (ZIF-8) based polymer nanocomposite membranes for gas separation", Energy Environ. Sci. 5 (2012), 8359.

[21] T. Li, Y. Pan, K.-V. Peinemann, Z. Lai, "Carbon dioxide selective mixed matrix composite membrane containing ZIF-7 nano-fillers", J. Membr. Sci. 425-426 (2013) 235–242.

[22] Surendar R. Venna and Moises A. Carreon, "Highly Permeable Zeolite Imidazolate Framework-8 Membranes for CO_2/CH_4 Separation", J. Am. Chem. Soc. (2010), 132, 76–78.

[23] L. Ge, W. Zhou, A. Du, and Z. Zhu, "Porous Polyethersulfone-Supported Zeolitic Imidazolate Framework Membranes for Hydrogen Separation", J. Phys. Chem. C 116 (2012), 13264−13270.

[24] Ma. Josephine C. Ordoñez, "Gas Permeability and Selectivity Properties of ZIF-8/Matrimid® Mixed-Matrix Membranes", MS Thesis, The University of Texas, Dallas (2009).

[25] Uyen P. N. Tran, Ky K. A. Le, and Nam T. S. Phan, "Expanding Applications of Metal-Organic Frameworks: Zeolite Imidazolate Framework ZIF-8 as an Efficient Heterogeneous Catalyst for the Knoevenagel Reaction", ACS Catal. 1 (2011), 120–127.

[26] S. Basu, A. Cano-Odena, I. F. J. Vankelecom, "MOF-containing mixed-matrix membranes for CO_2/CH_4 and CO_2/N_2 binary gas mixture separations", Sep. Purif. Technol 81 (2011), 31–40.